

Audiovisual biofeedback improves the correlation between internal/external surrogate motion and lung tumor motion

Danny Lee^{1,2}, Peter B. Greer^{1,3}, Chiara Paganelli⁴, Joanna Ludbrook^{1,3}, Taeho Kim⁵ and Paul Keall²

¹*School of Mathematical and Physical Sciences, The University of Newcastle, NSW, Australia.*

5 ²*Radiation Physics Laboratory, Sydney Medical School, University of Sydney, NSW, Australia*

³*Department of Radiation Oncology, Calvary Mater Newcastle, NSW, Australia.*

⁴*Dipartimento di Elettronica, Informazione e Bioingegneria, Politecnico di Milano, Italy.*

⁵*Department of Radiation Oncology, Virginia Commonwealth University, Richmond, VA, US.*

10 Corresponding Author: Paul Keall, Ph.D.

Radiation Physics Laboratory, Sydney Medical School, University of Sydney

Room 475, Blackburn Building D06

The University of Sydney

NSW Australia 2006

15 (phone): 61 2 9351 3385 (fax): 61 2 9351 4018

e-mail: paul.keall@sydney.edu.au

ABSTRACT

20 **Purpose:** Breathing management can reduce breath-to-breath (intra-fraction) and day-by-day (inter-fraction) variability in breathing motion whilst utilizing the respiratory motion of internal and external surrogates for respiratory guidance. Audiovisual (AV) biofeedback, an interactive personalized breathing motion management system, has been developed to improve reproducibility of intra- and inter-fraction breathing motion. However, the assumption of the correlation of respiratory motion between surrogates and tumors is not always verified
25 during medical imaging and radiation treatment. Therefore, the aim of the study was to test the hypothesis that the correlation of respiratory motion between surrogates and tumors is the same under free breathing without guidance (FB) and with AV biofeedback guidance for voluntary motion management.

Methods: For 13 lung cancer patients receiving radiotherapy, 2D coronal and sagittal cine-MR images were acquired across two MRI sessions (pre- and mid-treatment) with two breathing conditions: (1) FB and (2) AV
30 biofeedback, totaling eighty-eight patient measurements. Simultaneously, the external respiratory motion of the abdomen was measured. The internal respiratory motion of the diaphragm and lung tumor was retrospectively measured from 2D coronal and sagittal cine-MR images. The correlation of respiratory motion between surrogates and tumors was calculated using Pearson's correlation coefficient for: (1) abdomen to tumor (abdomen-tumor) and (2) diaphragm to tumor (diaphragm-tumor). The correlations were compared between FB
35 and AV biofeedback using several metrics: abdomen-tumor and diaphragm-tumor correlations with/without ≥ 5 mm tumor motion range and with/without adjusting for phase shifts between the signals.

Results: Compared to FB, AV biofeedback improved abdomen-tumor correlation by 11% ($p=0.12$) from 0.53 to 0.59 and diaphragm-tumor correlation by 13% ($p=0.02$) from 0.55 to 0.62. Compared to FB, AV biofeedback improved abdomen-tumor correlation by 17% ($p=0.01$) and diaphragm-tumor correlation by 15% ($p<0.01$)
40 whilst correcting 0.3 s ($p=0.54$) and 0.2 s ($p=0.19$) phase shifts, respectively. In addition, AV biofeedback with ≥ 5 mm tumor motion range, compared to FB improved abdomen-tumor correlation by 14% ($p=0.18$) and diaphragm-tumor correlation by 17% ($p=0.01$). The highest abdomen-tumor and diaphragm-tumor correlations were found using ≥ 5 mm tumor motion range and phase shifts, resulting in a 12% improvement in AV biofeedback.

45 **Conclusions:** Our results demonstrated that AV biofeedback improves the correlation of respiratory motion between surrogates and the tumor. This suggests a need for AV biofeedback for respiratory guidance utilizing respiratory surrogates during image-guided and MRI-guided radiotherapy in thoracic regions.

Keywords: audiovisual biofeedback; motion correlation; tumor motion; respiratory guidance; respiratory motion

50 **I. INTRODUCTION**

Breathing variations^{1,2} can cause image artifacts^{3,4} and blurring of dose distributions^{5,6} during medical imaging and lung cancer radiotherapy. To overcome this issue, breathing management can reduce breath-to-breath (intra-fraction) and day-to-day (inter-fraction) variability whilst utilizing respiratory signals for respiratory guidance.^{5,7,8}

55 Respiratory surrogates are often used to predict tumor motion during breathing and compensate for tumor motion with respiratory gating and tracking, and to derive system latency between tumor positioning and radiation delivery.⁹⁻¹² However, tumor motion is not always accurately correlated to the internal/external surrogates due to breathing and heartbeat.¹³⁻¹⁵ In order to avoid mis-targeting during respiratory-gated imaging and radiotherapy, the correlation between internal/external surrogates and tumor motion needs to be
60 addressed.^{13,16,17}

Interactive personalized breathing management systems such as audiovisual (AV) biofeedback have been developed to improve reproducibility of intra- and inter-fraction breathing motion. Specifically, Kini *et al.* (2003)⁷ demonstrated that an audio biofeedback (i.e. “breathe in” or “breathe out” at periodic intervals) can improve the reproducibility in the period of the breathing motion, and visual feedback using a bar model can
65 improve the reproducibility in the displacement of the breathing motion. George *et al.* (2006)⁸ combined an audio biofeedback with a bar model for AV biofeedback, thus significantly reducing residual motion. In addition, Venkat *et al.* (2008) proposed a wave model composed by an average of ten individual breathing cycles and demonstrated its superior performance on a volunteer study in 0.8 mm and 0.2 s with respect to the bar model.¹⁸ AV biofeedback was also employed by Cui *et al.* (2010)¹⁹ to improve patients’ respiratory
70 regularity during 4DCT image acquisition, in order to avoid the artifacts in 4DCT images caused by intra-fraction irregular breathing and allow improved dose delivery accuracy during radiotherapy. Kim *et al.* (2012)²⁰ and Lee *et al.* (2016)²¹ employed AV biofeedback to improve the reproducibility of diaphragm and lung tumor motion measured in MRI. Intra-fraction diaphragm motion reproducibility was improved by 38% in displacement and 82% in a breathing period,²⁰ and intra and inter-fraction tumor motion reproducibility was
75 improved by 34% and 42% in displacement and 73% and 74% in a breathing period,²¹ by using AV biofeedback with respect to a free-breathing acquisition.

Although it has been demonstrated that AV biofeedback^{7,8,18-21} improves breathing motion reproducibility, it has been conjectured that this improvement might be offset by lower surrogate to tumor correlation, as the act of biofeedback affects how the patient breathes. A previous study²² on healthy subjects found that the

80 correlation of respiratory motion between internal and external surrogates (diaphragm and abdomen) was the same with free breathing (FB) and AV biofeedback breathing. However, no patient studies have investigated this correlation and the volunteer study did not consider analysis with respect to motion directions and of the effects of phase shifts on the correlation. The current study therefore tested the hypothesis that the correlation of respiratory motion between internal/external surrogates and tumor is the same with FB and AV biofeedback
85 breathing for lung cancer patients. In addition, the effects of phase shifts and tumor motion range on correlations were investigated along with the variation in correlations between pre- and mid-treatment.

II. METHODS

90 The following sections describe the acquisition of respiratory-induced motion signals, their synchronization based on acquisition time and retrospective data analysis by quantifying the correlation of respiratory motion between surrogates and tumors.

II.A. Respiratory-induced motion signal acquisition

95 Thirteen lung cancer patients (non-small-cell and small-cell lung cancers with stage I–IIIB of any histology and a prescription dose of 40–60 Gy for primary lung cancer) were enrolled in a study approved by the Hunter New England Human Research Ethics Committee. The study used eighty-eight coronal and sagittal cine MR image datasets acquired with FB and AV biofeedback, which included fifty-two datasets from eight lung cancer patients obtained in a previous study.²¹ A 3 Tesla MRI scanner (Skyra, Siemens Healthcare Erlangen, Germany)
100 was used for coronal and sagittal cine-MRI in pre- and mid-treatment (i.e. three to six weeks after the pre-treatment). MRI scans were performed with arms down and head-first supine position. Nine patients completed both the first and second MRI sessions and the other three patients withdrew from the study after the first MRI session. Simultaneously, external respiratory signals were measured using a physiological measurement unit (PMU, A 3 Tesla MRI (Skyra, Siemens Healthcare Erlangen, Germany)) at the chest and a real-time position
105 management system (Varian, Palo Alto, USA) at the abdomen. The acquisition of internal/external respiratory-induced motion signals in AV biofeedback is shown in Figure 1.

The workflow of AV biofeedback²¹ is comprised of three steps (see Figure 1(a)): (1) an individual breathing pattern is obtained using external respiratory signals from RPM whilst monitoring the marker block on the

110 patient's abdomen, (2) the breathing pattern is displayed on the patient's visual display using a head-mounted-
mirror and screen in the MRI room, and (3) the patient controls their breathing in inhale and exhale breathing
displacement and period. The setup of the RPM block and camera was consistent during MRI sessions with both
FB and AV, and also it was consistent across the first and second MRI sessions. Specifically, the RPM block
and camera were located 2 cm below the navel due to a 32 channel body coil covers the entire chest and partial
115 abdomen and at the end of the MRI couch, respectively.²¹

Cine-MR images (see Figure 1(a)) and external-PMU signals (see Figure 1(b)) were simultaneously
obtained at 3.3 Hz and 400 Hz. This was repeated four times in each MRI session (coronal and sagittal cine-
MRI with FB and with AV biofeedback). Meanwhile, external-RPM signals were continuously obtained at 25
Hz during each MRI session. Then, respiratory motion of the diaphragm (i.e. liver dome)²⁰ and lung tumor (i.e.
120 the centroid of tumor contours)²¹ was directly measured from individual cine-MR images.²¹

II.B. Respiratory motion synchronization

In this study, respiratory motion from multi-modal systems was synchronized by comparing individual time
stamps, implemented in Matlab version 8.6.0 (The MathWorks, Natick, USA). The synchronization of the
125 respiratory motion was comprised of three steps.

- (1) Each external-PMU signal dataset (i.e. four datasets per MRI session) was synchronized by matching
its first acquisition time point to the corresponding first time point of external-RPM signals and also its
duration to the same duration of external-RPM signals, thus aligning external-PMU signals with
respect to external-RPM signals. In this study, external-RPM signals were the only signals used for
130 external abdominal motion because they provided absolute displacement in millimeters. PMU signals
provided the motion displacement in an arbitrary unit, which was not sensitive to a baseline drift in
displacement, but it was sufficient to synchronize two respiratory motions without mismatch.
- (2) Diaphragm and lung tumor motion was directly measured on coronal and sagittal cine-MR images.^{20, 21}
Lung tumor was automatically contoured using a region growing algorithm and its centroid was used
135 for measuring tumor motion.²¹ Diaphragm motion was also automatically measured at the peak of liver
dome scout.²² Thus, respiratory motions of diaphragm, abdomen and tumor had the same time point
and duration.
- (3) Diaphragm and tumor motion was linearly interpolated from 3.3 Hz to 25 Hz for further correlation
calculation, as well as the frequency of abdomen motion (25 Hz).

140 Respiratory motions of abdomen, diaphragm and tumor were described by (i) the abdomen motion in the anterior-posterior (AP) direction, (ii) the diaphragm motion in the superior-inferior direction (SI), (iii) the tumor motion in SI and left-right (LR) directions (i.e. tumor motion from coronal images) and (iv) the tumor motion in AP and SI motion (i.e. tumor motion from sagittal images).

145 **II.C. Data analysis**

The correlation between two nominated respiratory motions without smoothing was computed by using the Pearson's correlation coefficient in the linear relationship of displacement along the acquisition time. Correlations were investigated by quantifying:

- 150 (1) The correlation of respiratory motion between surrogates (abdominal-tumor and diaphragm-tumor) and tumor motion across eighty-eight coronal and sagittal datasets.
 - a. Abdomen motion (AP) to tumor motion (SI and LR) for coronal datasets.
 - b. Abdomen motion (AP) to tumor motion (AP and SI) for sagittal datasets.
 - c. Diaphragm motion (SI) to tumor motion (SI and LR) for coronal datasets.
 - d. Diaphragm motion (SI) to tumor motion (AP and SI) for sagittal datasets.
- 155 (2) Repeated (1) whilst correcting phase shifts (i.e. shifting one time series versus the other one to find the highest correlation via correcting displacement mismatch). In order to correct phase shifts, the larger displacement of two tumor motions (i.e. SI or LR for coronal datasets, and AP or SI for sagittal datasets) was applied to the other tumor motion for a consistent phase shift in each coronal and sagittal dataset.
- 160 (3) Repeated (1) with seventy-two datasets for a comparison of the correlation between pre- and mid-treatment from nine patients completed both the first and second MRI sessions.
- (4) Repeated (1) with sixty-eight datasets (≥ 5 mm tumor motion range).
- (5) Repeated (2) with sixty-eight datasets (≥ 5 mm tumor motion range) adjusted for phase shifts.

165 The correlation of respiratory motion between surrogates and tumors was individually computed for the four conditions above. The phase shifts were also measured for the second and fourth conditions. Positive (i.e. the same motion direction) and negative (i.e. the opposite motion direction) values were measured by the correlation of respiratory motion. To find the maximum correlation, the time series of respiratory-induced motion signal acquisitions shifted in a forward direction.

170 The mean of the phase shifts and absolute mean of correlations were reported along with the standard
 deviation (STD) and minimum/maximum values. The effects of AV feedback on correlations of tumor motion
 and phase shifts and the variation in pre and mid treatment correlations were compared using a Wilcoxon signed
 rank test with a 5% significance level.²³

175

III. RESULTS

Figure 2 shows an example of the respiratory motion measurements, abdomen (AP) obtained from the RPM
 system and diaphragm (SI), tumor (SI) and tumor (LR) motion obtained from a 2D coronal cine-MRI. Most
 tumors have a fairly small LR motion compared to SI and AP motion, however, an example of tumor with a
 180 large LR motion is shown in Figure 2.

The respiratory motion of surrogates can differ from the tumor motion in direction, period and phase (or
 time shift). The respiratory motions of the diaphragm SI (thick dotted line), tumor SI (thin solid line) and tumor
 LR (thin dotted line) move in the same direction but the respiratory motion of the abdomen AP (thick solid line)
 185 moves in the opposite direction. In addition, there is a small phase shift between diaphragm SI and tumor SI but
 a large phase shift for abdomen AP. A small phase shift can be also found between tumor SI and tumor LR.
 External motion at the abdomen is in the AP direction (thick solid line) and internal motion of the diaphragm is
 in the SI direction (thick dotted line). In other words, external motion reaches an anterior position (up) and
 internal motion reaches an inferior position (down) when the patients reaches inhalation.

190

Table 1 shows the correlation of respiratory motion between internal/external surrogates and tumors for 13
 lung cancer patients with multiple acquisition sessions.

Table 1. The correlation of respiratory motion between surrogates and tumors in a comparison between FB and AV
 biofeedback. Max correlation represents the highest correlation found in two tumor motion directions on 2D cine-MRI: (1)
 SI and LR directions on coronal images, and (2) SI and AP directions on sagittal images. A negative value indicates that
 surrogates and tumor move in the opposite direction. P: Patient, Cor: Coronal, Sag: Sagittal, S: MRI session, AV: AV
 biofeedback and *p*: a Wilcoxon signed rank test with absolute mean between FB and AV biofeedback.

Patients	Cine-MRI	Abdomen-tumor correlation						Diaphragm-tumor correlation					
		FB			AV			FB			AV		
		SI	LR/AP	Max	SI	LR/AP	Max	SI	LR/AP	Max	SI	LR/AP	Max

P01	S1	Cor	-0.79	-0.60	-0.79	-0.79	-0.38	-0.79	-0.76	-0.55	-0.76	-0.81	-0.39	-0.81
		Sag	-0.66	-0.52	-0.66	0.33	-0.73	-0.73	-0.66	-0.43	-0.66	0.25	-0.75	-0.75
P01	S2	Cor	-0.67	-0.08	-0.67	-0.73	-0.68	-0.73	-0.67	0.00	-0.67	-0.73	-0.63	-0.73
		Sag	0.08	0.23	0.23	-0.53	-0.74	-0.74	0.09	0.24	0.24	-0.50	-0.74	-0.74
P02	S1	Cor	-0.38	0.18	-0.38	0.31	-0.17	0.31	-0.26	0.12	-0.26	0.35	-0.27	0.35
		Sag	0.45	-0.66	-0.66	0.55	-0.06	0.55	0.41	-0.59	-0.59	0.60	-0.10	0.60
P02	S2	Cor	0.54	-0.01	0.54	-0.56	-0.08	-0.56	0.62	-0.04	0.62	0.68	-0.14	0.68
		Sag	0.68	0.56	0.68	0.67	0.39	0.67	0.66	0.54	0.66	0.76	0.39	0.76
P03	S1	Cor	0.40	-0.28	0.40	0.58	-0.33	0.58	0.41	-0.30	0.41	0.51	-0.40	0.51
		Sag	0.56	-0.55	0.56	0.72	-0.29	0.72	0.60	-0.59	0.60	0.86	-0.53	0.86
P04	S1	Cor	0.49	0.46	0.49	0.58	0.41	0.58	0.59	0.47	0.59	0.52	0.42	0.52
		Sag	0.51	-0.01	0.51	0.31	-0.42	-0.42	0.59	-0.07	0.59	0.45	-0.35	0.45
P05	S1	Cor	0.91	-0.69	0.91	0.89	-0.63	0.89	0.85	-0.57	0.85	0.88	-0.71	0.88
		Sag	0.93	-0.05	0.93	0.88	-0.41	0.88	0.92	-0.03	0.92	0.88	-0.57	0.88
P05	S2	Cor	0.80	-0.77	0.80	0.72	-0.49	0.72	0.50	-0.60	-0.60	0.71	-0.52	0.71
		Sag	0.44	-0.12	0.44	0.80	-0.56	0.80	0.91	-0.26	0.91	0.90	-0.66	0.90
P06	S1	Cor	0.65	-0.74	-0.74	0.55	-0.77	-0.77	0.65	-0.74	-0.74	0.57	-0.78	-0.78
		Sag	0.63	-0.59	0.63	0.65	-0.50	0.65	0.63	-0.70	-0.70	0.73	-0.57	0.73
P06	S2	Cor	0.64	-0.42	0.64	0.82	-0.60	0.82	0.74	-0.33	0.74	0.86	-0.69	0.86
		Sag	0.80	-0.65	0.80	0.81	-0.46	0.81	0.68	-0.49	0.68	0.77	-0.39	0.77
P07	S1	Cor	0.56	0.39	0.56	-0.34	0.83	0.83	0.51	0.38	0.51	-0.38	0.87	0.87
		Sag	-0.09	0.20	0.20	0.71	0.45	0.71	-0.03	0.24	0.24	0.54	0.29	0.54
P08	S1	Cor	0.33	0.36	0.36	0.29	0.47	0.47	0.30	0.41	0.41	0.27	0.47	0.47
		Sag	-0.27	-0.19	-0.27	0.18	-0.32	-0.32	-0.26	-0.16	-0.26	0.22	-0.33	-0.33
P08	S2	Cor	0.39	0.54	0.54	0.55	0.17	0.55	0.43	0.51	0.51	0.55	0.13	0.55
		Sag	0.09	-0.69	-0.69	-0.37	-0.32	-0.37	0.19	-0.61	-0.61	-0.37	-0.31	-0.37
P09	S1	Cor	0.49	-0.24	0.49	0.77	-0.39	0.77	0.56	-0.27	0.56	0.76	-0.44	0.76
		Sag	0.59	-0.12	0.59	0.70	0.30	0.70	0.61	-0.01	0.61	0.85	0.18	0.85
P09	S2	Cor	0.39	-0.09	0.39	0.64	-0.28	0.64	0.49	-0.01	0.49	0.77	-0.29	0.77
		Sag	0.38	0.23	0.38	0.72	0.67	0.72	0.40	0.32	0.40	0.78	0.69	0.78
P10	S1	Cor	0.32	0.14	0.32	0.47	-0.14	0.47	0.25	0.10	0.25	0.54	-0.15	0.54
		Sag	0.54	-0.32	0.54	0.54	0.49	0.54	0.53	-0.38	0.53	0.58	0.52	0.58
P10	S2	Cor	0.27	-0.04	0.27	0.47	0.27	0.47	0.33	-0.05	0.33	0.49	0.21	0.49
		Sag	0.43	-0.34	0.43	0.38	-0.34	0.38	0.40	-0.27	0.40	0.39	-0.42	-0.42
P11	S1	Cor	0.84	0.64	0.84	0.80	0.21	0.80	0.80	0.53	0.80	0.80	0.22	0.80
		Sag	0.58	0.36	0.58	0.70	0.07	0.70	0.70	0.36	0.70	0.80	-0.20	0.80
P12	S1	Cor	0.63	0.16	0.63	0.37	-0.26	0.37	0.71	0.08	0.71	0.66	-0.41	0.66
		Sag	0.25	0.53	0.53	0.37	0.31	0.37	0.40	0.41	0.41	0.35	0.34	0.35
P12	S2	Cor	0.73	-0.54	0.73	0.55	-0.25	0.55	0.75	-0.62	0.75	0.56	-0.20	0.56

	Sag	0.45	0.22	0.45	0.55	-0.01	0.55	0.52	0.23	0.52	0.60	-0.03	0.60	
P13	S1	Cor	0.16	-0.01	0.16	0.14	0.21	0.21	0.00	0.14	0.14	0.22	0.20	0.22
	Sag	0.31	0.00	0.31	0.35	-0.02	0.35	0.48	0.00	0.48	0.36	-0.02	0.36	
P13	S2	Cor	-0.06	-0.36	-0.36	0.02	0.06	0.06	-0.06	-0.33	-0.33	0.01	0.16	0.16
	Sag	0.30	-0.10	0.30	-0.37	-0.04	-0.37	0.42	-0.19	0.42	-0.37	-0.09	-0.37	
	Min/Max		-0.79/0.93		-0.79/0.89			-0.76/0.92			-0.81/0.90			
	Absolute mean		0.53		0.59			0.55			0.62			
	STD		0.49		0.54			0.52			0.54			
	<i>p</i>		= 0.12				= 0.02							

195 The correlation of abdomen-tumor with AV biofeedback in Table 1 ranged from -0.79 to 0.89 and FB from -0.79 to 0.93 whilst the correlation of diaphragm-tumor with AV biofeedback varied between -0.81 and 0.90, and FB between -0.76 and 0.92. Compared to FB, the absolute mean correlation with AV biofeedback was improved by 11% ($p=0.12$) from 0.53 to 0.59 in abdomen-tumor and 13% ($p=0.02$) from 0.55 to 0.62 in diaphragm-tumor. Of the surrogate-tumor correlations, the diaphragm-tumor correlation was higher than the abdomen-tumor correlation with both AV biofeedback and FB.

200

Table 2 shows the correlation of abdomen-tumor and diaphragm-tumor whilst correcting phase shifts.

Table 2. The correlation of abdomen-tumor and diaphragm-tumor with adjusted phase shifts. *p*: a Wilcoxon signed rank test with the absolute mean value for the correlation and the mean value for the phase shifts between FB and AV biofeedback.

Quantitative comparison		Abdomen-tumor correlation		Diaphragm-tumor correlation	
		FB	AV	FB	AV
Correlation	Min/Max	-0.82/0.96	-0.85/0.96	-0.82/0.93	-0.86/0.92
	Absolute mean	0.62	0.68	0.62	0.68
	STD	0.60	0.50	0.58	0.47
	<i>p</i>	= 0.01		< 0.01	
Phase shifts (s)	Min/Max	0.08/1.80	0.08/1.45	0.04/0.68	0.04/0.36
	Mean	0.32	0.30	0.20	0.17
	STD	0.32	0.28	0.13	0.09
	<i>p</i>	= 0.54		= 0.19	

The time series of surrogates were shifted to find the maximum correlation with the tumor. The means of the adjusted phase shifts were measured at 0.3 s for abdomen-tumor and 0.2 s for diaphragm-tumor. These phase

205 shifts resulted in a 17% higher correlation from 0.53 (see Table 1) to 0.62 with FB and a 15% higher correlation
 from 0.59 (see Table 1) to 0.68 with AV biofeedback for the abdomen-tumor correlation. Similarly they resulted
 in a 13% higher correlation from 0.55 (see Table 1) to 0.62 with FB and a 10% higher correlation from 0.62 (see
 Table 1) to 0.68 with AV biofeedback for the diaphragm-tumor correlation. For both FB and with AV
 biofeedback, the correlation for abdomen-tumor was the same as the correlation for diaphragm-tumor, however,
 210 AV biofeedback produced a 10% higher correlation for surrogate-tumor compared with FB alone.

Table 3 shows the correlation of abdomen-tumor and diaphragm-tumor with adjusted phase shifts across
 pre- and mid-treatment. Seventy-two of eighty-eight acquisitions from nine patients except for P03, P04 and
 P06 (see Table 1) were analyzed to compare variability on the correlation across pre- and mid-treatment. There
 215 was no significant difference in the correlations between pre- and mid-treatment, which indicates that the
 correlation of abdomen-tumor and diaphragm-tumor does not significantly vary across the two MRI sessions
 with both FB and AV biofeedback.

Table 3. The correlation of abdomen-tumor and diaphragm-tumor with adjusted phase shifts across pre- and mid-
 treatment. Pre: pre-treatment, Mid: mid-treatment, Both: pre- and mid-treatment, and p : a Wilcoxon signed rank
 test between pre- and mid-treatment.

Quantitative comparison	Abdomen-tumor correlation						Diaphragm-tumor correlation						
	FB			AV			FB			AV			
	Pre	Mid	Both	Pre	Mid	Both	Pre	Mid	Both	Pre	Mid	Both	
Correlation	Min	-0.78	-0.77	-0.78	-0.85	-0.54	-0.85	-0.76	-0.74	-0.76	-0.86	-0.48	-0.86
	/Max	/0.96	/0.95	/0.96	/0.93	/0.96	/0.96	/0.93	/0.91	/0.93	/0.88	/0.92	/0.92
	Absolute mean	0.65	0.59	0.62	0.65	0.67	0.65	0.62	0.63	0.62	0.67	0.68	0.67
	STD	0.61	0.56	0.58	0.52	0.46	0.57	0.59	0.54	0.49	0.58	0.35	0.49
	p	= 0.96			= 0.52			= 0.64			= 0.14		
Phase shifts (s)	Min	0.08	0.08	0.08	0.08	0.08	0.08	0.04	0.04	0.04	0.04	0.04	0.04
	/Max	/1.06	/1.80	/1.80	/0.92	/1.45	/1.45	/0.32	/0.44	/0.44	/0.36	/0.36	/0.36
	Mean	0.27	0.35	0.31	0.31	0.33	0.32	0.17	0.20	0.19	0.18	0.16	0.17
	STD	0.26	0.42	0.34	0.25	0.39	0.31	0.10	0.13	0.11	0.11	0.09	0.10
	p	= 0.08			= 0.60			= 0.20			= 0.40		

Figure 3 shows the correlation of respiratory motion between surrogates and tumor from sixty-eight
 220 acquisitions with ≥ 5 mm tumor motion range. Absolute correlation values were used to demonstrate a

comparison of its (higher or lower) correlation between FB and AV biofeedback across abdomen-tumor and diaphragm-tumor.

In the correlation two subgroups between sixty-eight datasets (≥ 5 mm tumor motion range) and eighty-eight datasets (> 0 mm tumor motion range), AV biofeedback, compared to FB, improved abdomen-tumor correlation by 14% ($p=0.18$) from 0.57 to 0.65 and diaphragm-tumor correlation by 17% ($p=0.01$) from 0.59 to 0.69. In addition, the correlations from the acquisitions with ≥ 5 mm tumor motion were compared to the correlations from all datasets in Table 1. Higher correlations were observed with ≥ 5 mm tumor motion with FB by 8% of abdomen-tumor correlation from 0.53 to 0.57 and 7% of diaphragm-tumor correlation from 0.55 to 0.59, and also with AV biofeedback, 10% of abdomen-tumor correlation from 0.59 to 0.65 and 11% of diaphragm-tumor correlation from 0.62 to 0.69.

Table 4 shows the correlation of abdomen-tumor and diaphragm-tumor with adjusted phase shifts and ≥ 5 mm tumor motion range.

Table 4. The correlation of abdomen-tumor and diaphragm-tumor with adjusted phase shifts and ≥ 5 mm tumor motion range. p : a Wilcoxon signed rank test between FB and AV biofeedback.

Quantitative comparison		Abdomen-tumor correlation		Diaphragm-tumor correlation	
		FB	AV	FB	AV
Correlation	Min/Max	-0.82/0.96	-0.85/0.96	-0.82/0.93	-0.85/0.92
	Absolute mean	0.67	0.75	0.68	0.76
	STD	0.62	0.46	0.61	0.45
p		= 0.02		< 0.01	

235

With ≥ 5 mm tumor motion range, the phase shift produced higher correlations in both abdomen-tumor and diaphragm-tumor correlations, 8% ($p=0.02$) from 0.62 (see Table 2) to 0.67 and 10% ($p<0.01$) from 0.62 (see Table 2) to 0.68 improvements in FB and AV biofeedback, respectively. With a minimal increase of phase shifts, an average of 2 – 3 milliseconds (see Table 2), the abdomen-tumor and diaphragm-tumor correlations were similarly improved in both FB and AV biofeedback but remained 12% higher with AV biofeedback compared with FB alone.

240

IV. DISCUSSION

245 Lung tumor displacement and baseline drift due to intra- and inter-fraction breathing motion variability, may lead to a failure in accurate radiation delivery and tumor motion predictions.^{9, 12} Most breathing management techniques rely on internal and external surrogates to improve tumor motion controlled and predictions, but the respiratory motion of surrogates does not always accurately match tumor motion.

In the literature, the AV biofeedback system has been shown to improve the reproducibility of breathing motion with respect to FB,²⁴ and an internal/external correlation between FB and AV biofeedback was found to be consistent for healthy volunteers.²² However, no studies on the correlation between surrogate and tumor motion with AV biofeedback have been reported. Therefore, in this study, we used MR images to study the correlation of respiratory motion between the surrogates and the tumors with and without AV biofeedback. As shown in Table 1, for all the acquired patients over different sessions, the correlation between the analyzed surrogates (i.e. abdomen and diaphragm) and the tumor motion increased over 10% with AV biofeedback in comparison to the standard FB acquisition. This correlation can be additionally improved by compensating for phase shifts to allow the maximum correlation (see Table 2). The phase shifts for FB and AV biofeedback appeared to be similar, but slightly smaller with AV than FB. In this case, the correlation increased in FB and AV biofeedback for both abdomen-tumor and diaphragm-tumor pairs. Specifically, the phase shifts were 0.3 s for abdomen-tumor and 0.2 s for diaphragm-tumor, suggesting the need to compensate for these time discrepancies in order to further improve respiratory gating and tracking efficacy and tumor motion predictions. In this study, MRI scans were performed with arms down and head-first supine position. However, we believe that even with arms up, AV feedback could potentially improve the correlation between internal/external surrogate motion and lung tumor motion and future studies could investigate the impact of AV biofeedback with different patient positions.

The positive effect of AV biofeedback with respect to FB in improving the correlation of tumor motion with surrogates is apparent on patients with a larger range of motion (≥ 5 mm),¹⁰ suggesting the potential utility of AV biofeedback for patients with a high range of motion. This is due to correlation being affected by (1) breathing motion consistency in displacement and period, and (2) tumor motion large enough to clearly distinguish each cycle. This study demonstrated higher correlation when tumor motion is ≥ 5 mm due to less noisy respiratory motion.

The RPM system is often used to monitor breathing motion for acquiring time-resolved images and compensating breathing motion during thoracic imaging, and radiotherapy. In addition, RPM is widely used in

many clinics due to its superior accuracy with absolute displacement in sub-millimeters. However, RPM is an independent system to MRI so it is unable to be used to synchronize acquisition time between RPM signals and MR images. In this study, to synchronize RPM signal to the MR images the RPM was synchronized to the PMU system, which uses the time-base of the MRI scanner. So far, only two MRI studies^{21, 22} have utilized RPM signals as inputs of breathing motion guidance because it requires an appropriate innovation in visual guidance with MR-compatible materials (i.e. a head-mounted mirror for providing visual guidance and a plastic transparent screen for displaying visual guidance with a projector). RPM can be replaced with other breathing motion monitoring devices which provide absolute displacement, and with a time-base synchronized to MR image acquisition.

Compared to the motion of internal and external surrogates, tumor motion varies in motion direction and phase shift. Thus it is very important that tumor motion is analyzed using 2D cine or 4D images prior to predicting tumor location and respiratory-gated radiotherapy. For example, if the tumor is located at (near) the chest wall, it moves in the direction of chest wall motion, which differs from diaphragm motion and is the same as abdominal motion. Thus, individual treatment plans can be customized to improve lung cancer radiotherapy outcome, whilst considering respiratory motion management using AV biofeedback. In addition, phase shifts between internal/external surrogates and tumors, and their motion direction should be considered to achieve a better correlation.

The limitations of the present study were that the diaphragm visibility was restricted on lung tumor images depending on the tumor location and the tumor displacement of some patients was considerably small (less than 2 mm) to distinguish tumor motion from noise, resulting in a tumor motion correlation lower than 0.2. Moreover, the respiratory motion of lung and abdominal tumors is dependent on tumor size, location and patient respiratory pattern.²⁵ However, the correlation of respiratory motion between surrogates and tumor and the subsequent effectiveness of the treatment can be further analyzed by selecting patients who may potentially require AV biofeedback integrated with clinically available and innovative image-guided tumor motion monitoring techniques, such as MRI-guidance.^{2, 26, 27}

Our results demonstrated that AV biofeedback significantly improved the correlation of respiratory motion between surrogates and tumor, thus suggesting the need for the integration of AV biofeedback into external beam radiotherapy.

V. CONCLUSIONS

305 This was the first study in which AV biofeedback was used to derive the correlation of respiratory motion
between surrogates and tumors, through the acquisition of fast cine-MRI slices. By utilizing audiovisual
biofeedback, we demonstrated an improvement of 11% in abdomen to tumor correlation and 13% in diaphragm
to tumor correlation with respect to a standard free-breathing acquisition, thus suggesting that AV biofeedback
could be a desirable technique for respiratory guidance during image-guided and MRI-guided radiotherapy in
310 thoracic and abdominal regions.

Acknowledgements

This project was supported by an NHMRC Australia Fellowship. We also thank the radiographers at the Calvary
315 Mater Newcastle and Department of Radiation Oncology for MRI research scan funding. We acknowledge and
appreciate the voluntary time of the patients without whom this study would not have been possible.

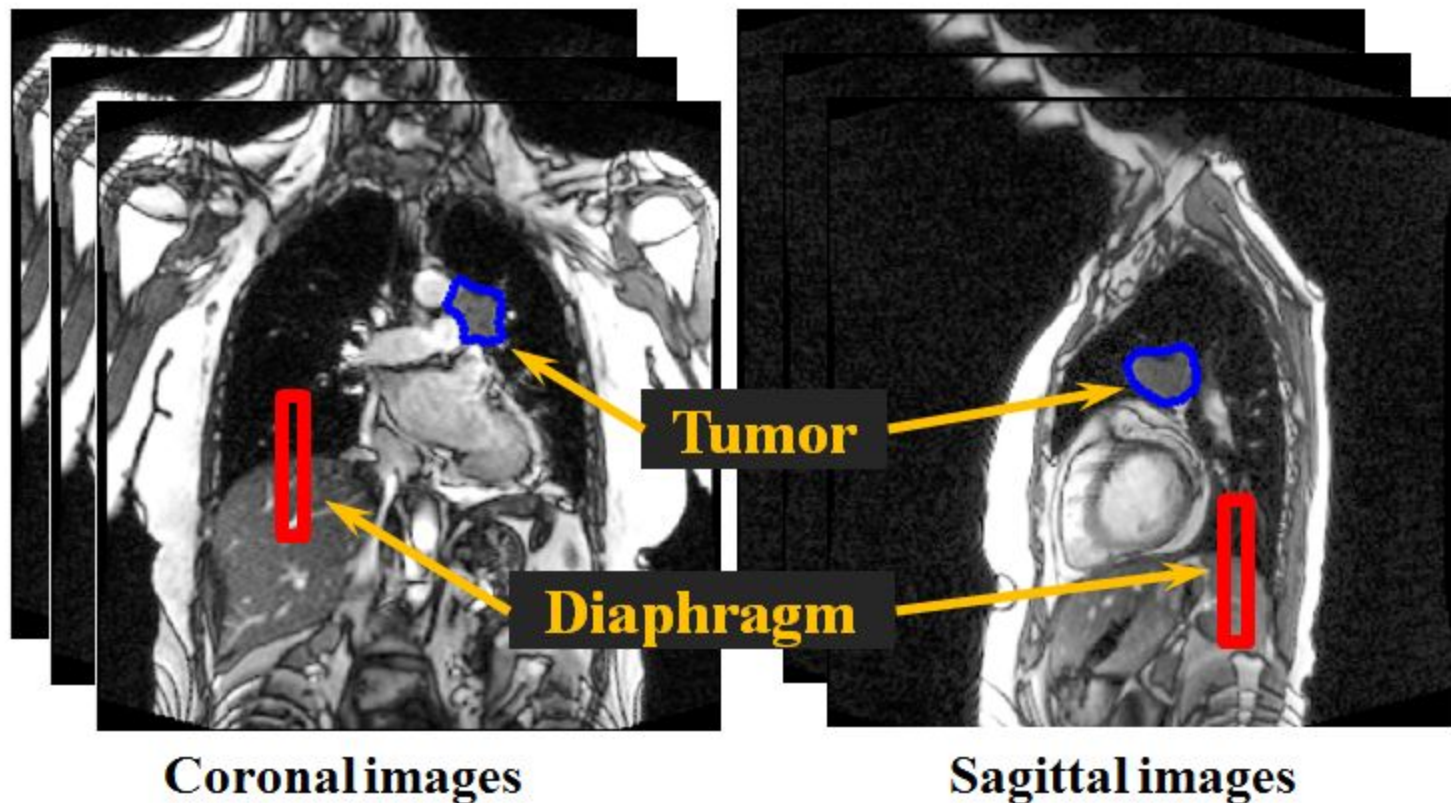
References

- 320 ¹ T.J. Nøttrup, S.S. Korreman, A.N. Pedersen, L.R. Aarup, H. Nyström, M. Olsen, L. Specht, "Intra-and
interfraction breathing variations during curative radiotherapy for lung cancer," *Radiotherapy and oncology*
84, 40-48 (2007).
- ² A.P. Shah, P.A. Kupelian, B.J. Waghorn, T.R. Willoughby, J.M. Rineer, R.R. Mañon, M.A. Vollenweider,
S.L. Meeks, "Real-time tumor tracking in the lung using an electromagnetic tracking system," *International*
325 *Journal of Radiation Oncology* Biology* Physics* **86**, 477-483 (2013).
- ³ T. Yamamoto, U. Langner, B.W. Loo, J. Shen, P.J. Keall, "Retrospective analysis of artifacts in four-
dimensional CT images of 50 abdominal and thoracic radiotherapy patients," *International Journal of*
Radiation Oncology Biology* Physics* **72**, 1250-1258 (2008).
- ⁴ D. Lee, P. Greer, J. Arm, P. Keall, T. Kim, presented at the *Journal of Physics: Conference Series* 2014
330 (unpublished).
- ⁵ J.M. Balter, R.K. Ten Haken, T.S. Lawrence, K.L. Lam, J.M. Robertson, "Uncertainties in CT-based
radiation therapy treatment planning associated with patient breathing," *International Journal of Radiation*
Oncology Biology* Physics* **36**, 167-174 (1996).
- ⁶ J. Ge, L. Santanam, C. Noel, P.J. Parikh, "Planning 4-dimensional computed tomography (4DCT) cannot
335 adequately represent daily intrafractional motion of abdominal tumors," *International Journal of Radiation*
Oncology Biology* Physics* **85**, 999-1005 (2013).
- ⁷ V.R. Kini, S.S. Vedam, P.J. Keall, S. Patil, C. Chen, R. Mohan, "Patient training in respiratory-gated
radiotherapy," *Medical Dosimetry* **28**, 7-11 (2003).
- ⁸ R. George, T.D. Chung, S.S. Vedam, V. Ramakrishnan, R. Mohan, E. Weiss, P.J. Keall, "Audio-visual
340 biofeedback for respiratory-gated radiotherapy: impact of audio instruction and audio-visual biofeedback on
respiratory-gated radiotherapy," *International Journal of Radiation Oncology* Biology* Physics* **65**, 924-933
(2006).
- ⁹ G.C. Sharp, S.B. Jiang, S. Shimizu, H. Shirato, "Prediction of respiratory tumour motion for real-time image-
guided radiotherapy," *Physics in medicine and biology* **49**, 425 (2004).
- 345 ¹⁰ P.J. Keall, G.S. Mageras, J.M. Balter, R.S. Emery, K.M. Forster, S.B. Jiang, J.M. Kapatoes, D.A. Low, M.J.
Murphy, B.R. Murray, "The management of respiratory motion in radiation oncology report of AAPM Task
Group 76," *Medical physics* **33**, 3874-3900 (2006).

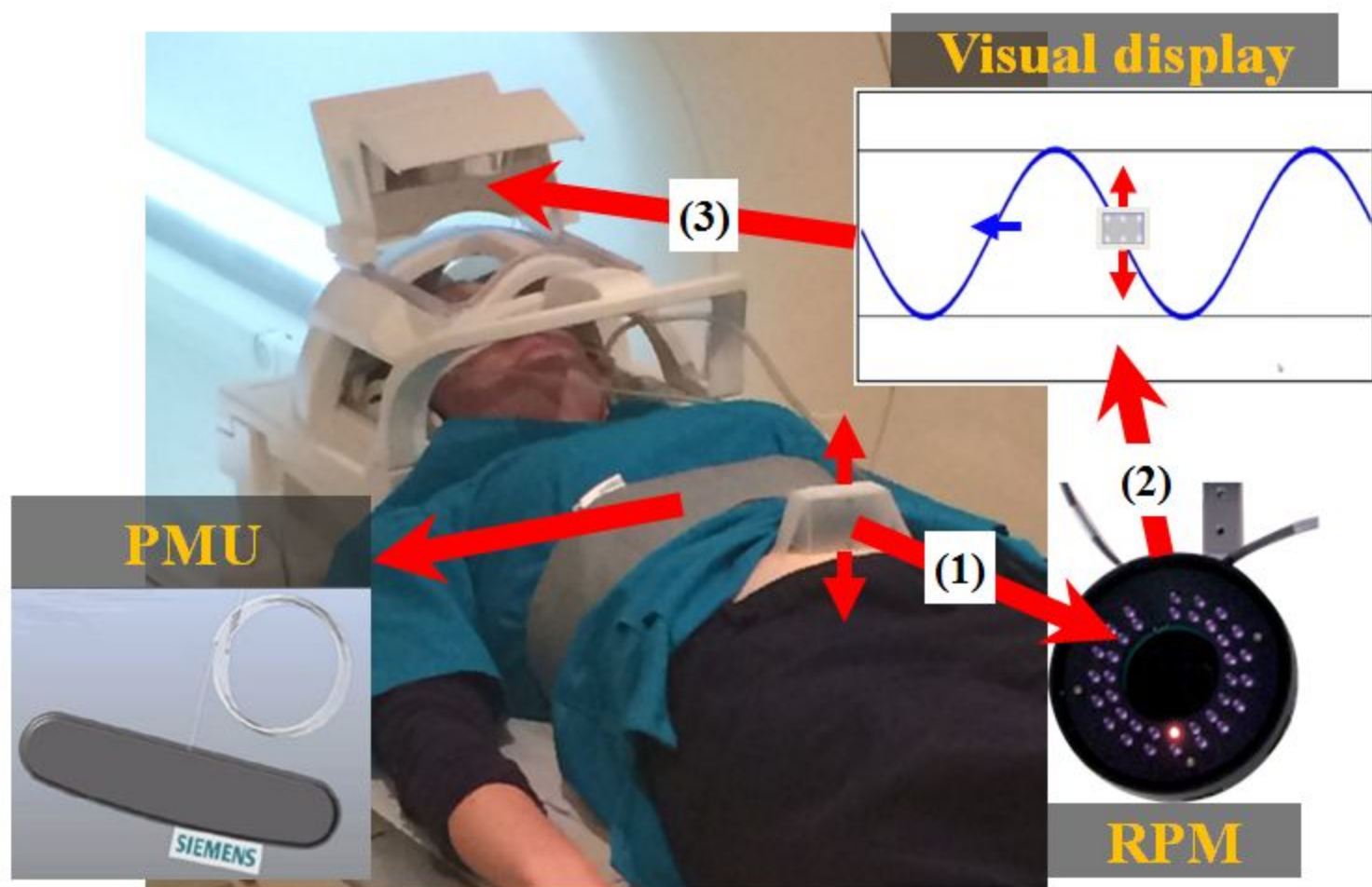
- 350 ¹¹ M. Seregni, C. Paganelli, D. Lee, P. Greer, G. Baroni, P. Keall, M. Riboldi, "Motion prediction in MRI-guided radiotherapy based on interleaved orthogonal cine-MRI," *Physics in medicine and biology* **61**, 872 (2016).
- ¹² T. Krilavicius, I. Zliobaite, H. Simonavicius, L. Jarusevicius, "Predicting respiratory motion for real-time tumour tracking in radiotherapy," arXiv preprint arXiv:1508.007492(2015).
- 355 ¹³ D.P. Gierga, J. Brewer, G.C. Sharp, M. Betke, C.G. Willett, G.T. Chen, "The correlation between internal and external markers for abdominal tumors: implications for respiratory gating," *International Journal of Radiation Oncology* Biology* Physics* **61**, 1551-1558 (2005).
- ¹⁴ Y. Seppenwoolde, H. Shirato, K. Kitamura, S. Shimizu, M. van Herk, J.V. Lebesque, K. Miyasaka, "Precise and real-time measurement of 3D tumor motion in lung due to breathing and heartbeat, measured during radiotherapy," *International Journal of Radiation Oncology* Biology* Physics* **53**, 822-834 (2002).
- 360 ¹⁵ D. Ionascu, S.B. Jiang, S. Nishioka, H. Shirato, R.I. Berbeco, "Internal-external correlation investigations of respiratory induced motion of lung tumors," *Medical physics* **34**, 3893-3903 (2007).
- ¹⁶ J.D. Hoisak, K.E. Sixel, R. Tirona, P.C. Cheung, J.-P. Pignol, "Correlation of lung tumor motion with external surrogate indicators of respiration," *International Journal of Radiation Oncology* Biology* Physics* **60**, 1298-1306 (2004).
- 365 ¹⁷ A.S. Beddar, K. Kainz, T.M. Briere, Y. Tsunashima, T. Pan, K. Prado, R. Mohan, M. Gillin, S. Krishnan, "Correlation between internal fiducial tumor motion and external marker motion for liver tumors imaged with 4D-CT," *International Journal of Radiation Oncology* Biology* Physics* **67**, 630-638 (2007).
- ¹⁸ R.B. Venkat, A. Sawant, Y. Suh, R. George, P.J. Keall, "Development and preliminary evaluation of a prototype audiovisual biofeedback device incorporating a patient-specific guiding waveform," *Physics in medicine and biology* **53**, N197 (2008).
- 370 ¹⁹ G. Cui, S. Gopalan, T. Yamamoto, J. Berger, P.G. Maxim, P.J. Keall, "Commissioning and quality assurance for a respiratory training system based on audiovisual biofeedback," *Journal of applied clinical medical physics/American College of Medical Physics* **11**, 3262 (2010).
- ²⁰ T. Kim, S. Pollock, D. Lee, R. O'Brien, P. Keall, "Audiovisual biofeedback improves diaphragm motion reproducibility in MRI," *Medical physics* **39**, 6921-6928 (2012).
- 375 ²¹ D. Lee, P.B. Greer, J. Ludbrook, J. Arm, P. Hunter, S. Pollock, K. Makhija, R.T. O'brien, T. Kim, P. Keall, "Audiovisual Biofeedback Improves Cine-Magnetic Resonance Imaging Measured Lung Tumor Motion Consistency," *International Journal of Radiation Oncology* Biology* Physics* **94**, 628-636 (2016).

- 380 ²² H. Steel, S. Pollock, D. Lee, P. Keall, T. Kim, "The internal–external respiratory motion correlation is unaffected by audiovisual biofeedback," *Australasian Physical & Engineering Sciences in Medicine* **37**, 97-102 (2014).
- ²³ J.D. Gibbons, S. Chakraborti, *Nonparametric statistical inference*. (Springer, 2011).
- ²⁴ S. Pollock, R. Keall, P. Keall, "Breathing guidance in radiation oncology and radiology: A systematic review of patient and healthy volunteer studies," *Medical physics* **42**, 5490-5509 (2015).
- 385 ²⁵ C.W. Stevens, R.F. Munden, K.M. Forster, J.F. Kelly, Z. Liao, G. Starkschall, S. Tucker, R. Komaki, "Respiratory-driven lung tumor motion is independent of tumor size, tumor location, and pulmonary function," *International Journal of Radiation Oncology* Biology* Physics* **51**, 62-68 (2001).
- ²⁶ S. Mutic, J.F. Dempsey, "The ViewRay System: Magnetic Resonance–Guided and Controlled Radiotherapy," *Seminars in radiation oncology* **24**, 196-199 (2014).
- 390 ²⁷ C. Paganelli, M. Seregini, G. Fattori, P. Summers, M. Bellomi, G. Baroni, M. Riboldi, "Magnetic resonance imaging–guided versus surrogate-based motion tracking in liver radiation therapy: a prospective comparative study," *International Journal of Radiation Oncology* Biology* Physics* **91**, 840-848 (2015).

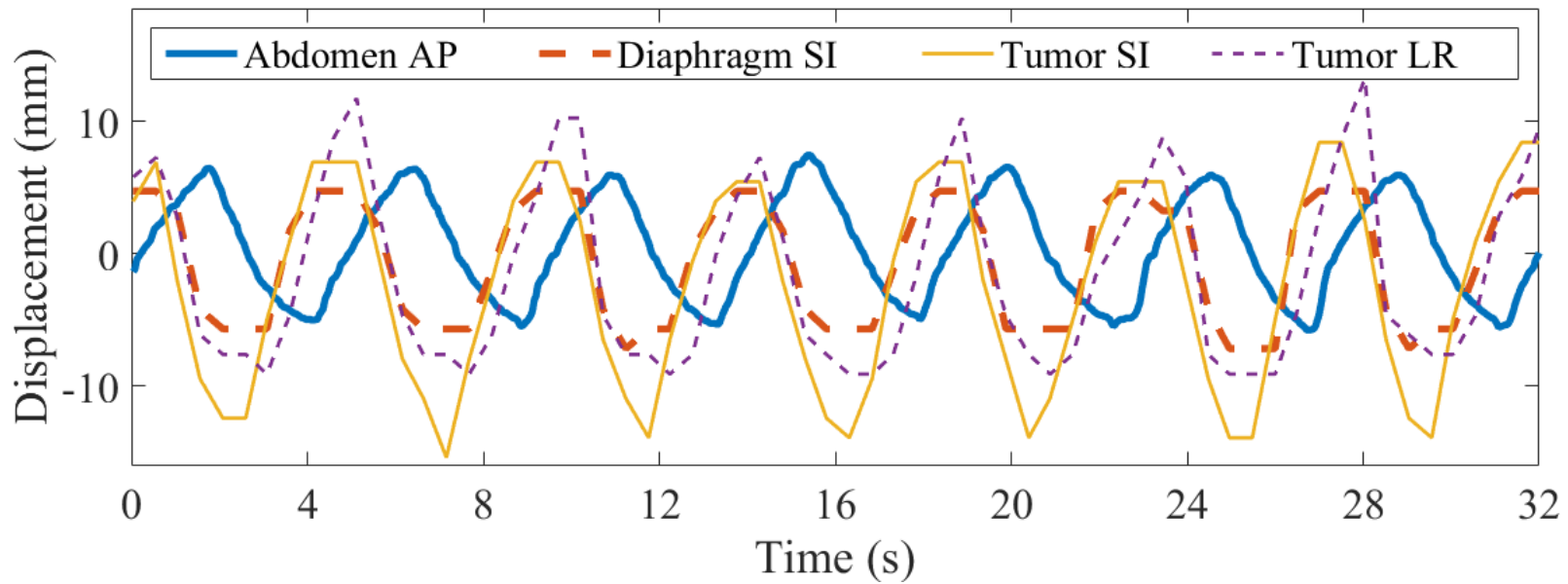
(a) Respiratory-induced internal motion measurements



(b) Respiratory-induced external motion measurements



Respiratory motion measurements



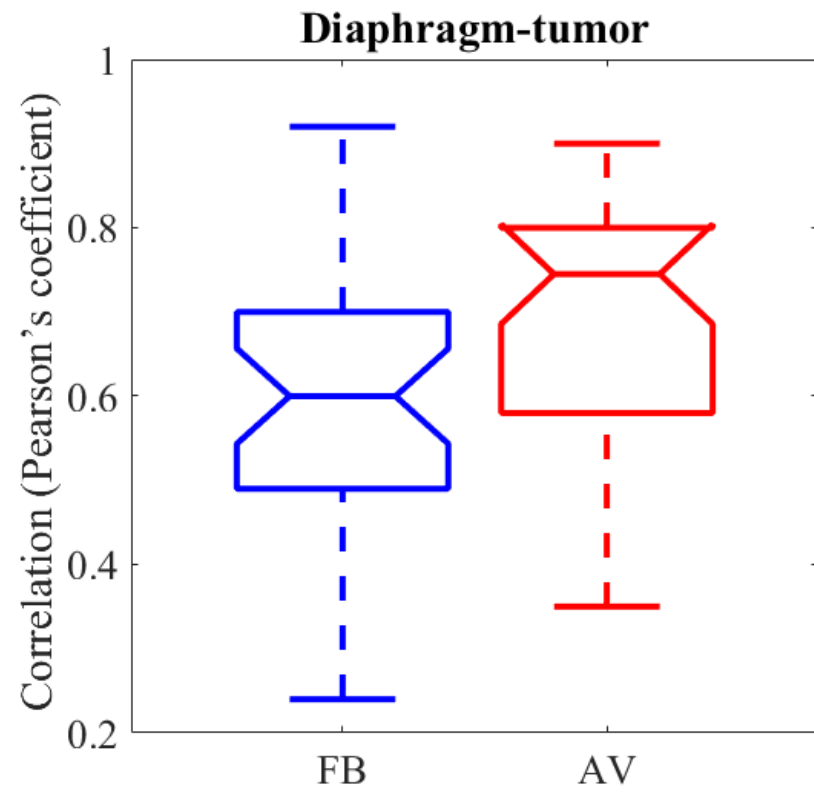
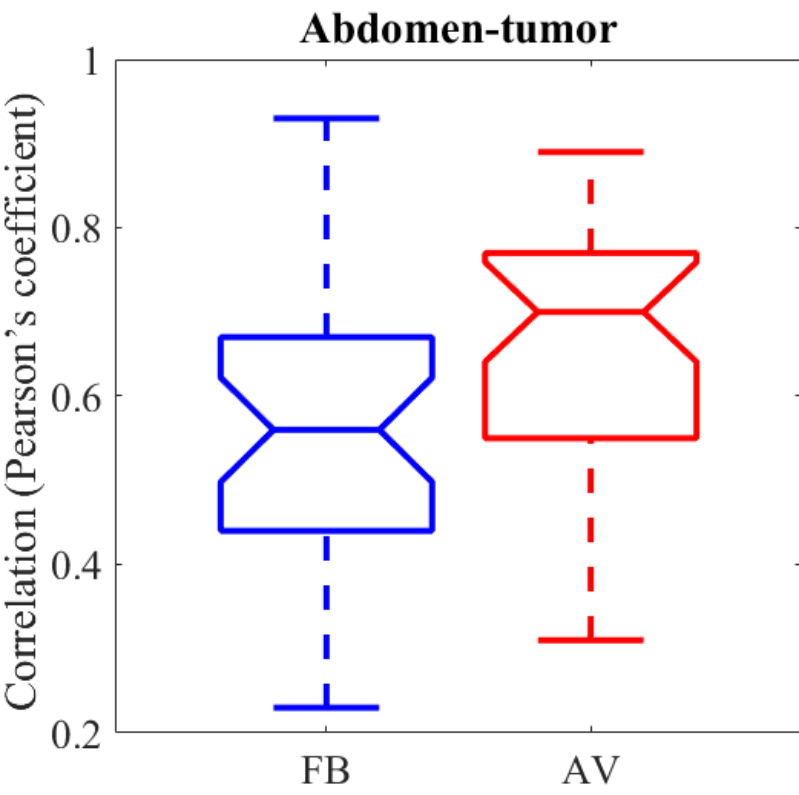


Figure 1. Respiratory-induced motion acquisitions in AV biofeedback: (a) internal diaphragm (vertical rectangle (red)) and lung tumor (circle (blue)) motion measurements, directly measured from coronal and sagittal cine-MR images, and (b) external chest and abdomen motion measurements.

Figure 2. An example respiratory motion obtained from the external measurement: abdomen AP (thick solid line) and internal measurements from 2D coronal cine-MRI: diaphragm SI (thick dotted line), tumor SI (thin solid line) and tumor LR (thin dotted line). The diaphragm SI motion is smaller than tumor SI and LR motions due to the tumor location close to the chest wall and back, where the diaphragm motion is limited on lung tumor images.

Figure 3. The correlation of abdomen-tumor and diaphragm-tumor with ≥ 5 mm tumor motion range. On each box, the central mark is the median, the edges of the box are the 25th and 75th percentiles, and the end lines after each dotted line extend to the most extreme data points.

Table 1. The correlation of respiratory motion between surrogates and tumors in a comparison between FB and AV biofeedback.

Max correlation represents the highest correlation found in two tumor motion directions on 2D cine-MRI: (1) SI and LR directions on coronal images, and (2) SI and AP directions on sagittal images. A negative value indicates that surrogates and tumor move in the opposite direction. P: Patient, Cor: Coronal, Sag: Sagittal, S: MRI session, AV: AV biofeedback and p : a Wilcoxon signed rank test with absolute mean between FB and AV biofeedback.

Patients	Cine-MRI	Abdomen-tumor correlation						Diaphragm-tumor correlation						
		FB			AV			FB			AV			
		SI	LR/AP	Max	SI	LR/AP	Max	SI	LR/AP	Max	SI	LR/AP	Max	
P01	S1	Cor	-0.79	-0.60	-0.79	-0.79	-0.38	-0.79	-0.76	-0.55	-0.76	-0.81	-0.39	-0.81
		Sag	-0.66	-0.52	-0.66	0.33	-0.73	-0.73	-0.66	-0.43	-0.66	0.25	-0.75	-0.75
P01	S2	Cor	-0.67	-0.08	-0.67	-0.73	-0.68	-0.73	-0.67	0.00	-0.67	-0.73	-0.63	-0.73
		Sag	0.08	0.23	0.23	-0.53	-0.74	-0.74	0.09	0.24	0.24	-0.50	-0.74	-0.74
P02	S1	Cor	-0.38	0.18	-0.38	0.31	-0.17	0.31	-0.26	0.12	-0.26	0.35	-0.27	0.35
		Sag	0.45	-0.66	-0.66	0.55	-0.06	0.55	0.41	-0.59	-0.59	0.60	-0.10	0.60
P02	S2	Cor	0.54	-0.01	0.54	-0.56	-0.08	-0.56	0.62	-0.04	0.62	0.68	-0.14	0.68
		Sag	0.68	0.56	0.68	0.67	0.39	0.67	0.66	0.54	0.66	0.76	0.39	0.76
P03	S1	Cor	0.40	-0.28	0.40	0.58	-0.33	0.58	0.41	-0.30	0.41	0.51	-0.40	0.51
		Sag	0.56	-0.55	0.56	0.72	-0.29	0.72	0.60	-0.59	0.60	0.86	-0.53	0.86
P04	S1	Cor	0.49	0.46	0.49	0.58	0.41	0.58	0.59	0.47	0.59	0.52	0.42	0.52
		Sag	0.51	-0.01	0.51	0.31	-0.42	-0.42	0.59	-0.07	0.59	0.45	-0.35	0.45
P05	S1	Cor	0.91	-0.69	0.91	0.89	-0.63	0.89	0.85	-0.57	0.85	0.88	-0.71	0.88
		Sag	0.93	-0.05	0.93	0.88	-0.41	0.88	0.92	-0.03	0.92	0.88	-0.57	0.88
P05	S2	Cor	0.80	-0.77	0.80	0.72	-0.49	0.72	0.50	-0.60	-0.60	0.71	-0.52	0.71
		Sag	0.44	-0.12	0.44	0.80	-0.56	0.80	0.91	-0.26	0.91	0.90	-0.66	0.90
P06	S1	Cor	0.65	-0.74	-0.74	0.55	-0.77	-0.77	0.65	-0.74	-0.74	0.57	-0.78	-0.78
		Sag	0.63	-0.59	0.63	0.65	-0.50	0.65	0.63	-0.70	-0.70	0.73	-0.57	0.73
P06	S2	Cor	0.64	-0.42	0.64	0.82	-0.60	0.82	0.74	-0.33	0.74	0.86	-0.69	0.86
		Sag	0.80	-0.65	0.80	0.81	-0.46	0.81	0.68	-0.49	0.68	0.77	-0.39	0.77
P07	S1	Cor	0.56	0.39	0.56	-0.34	0.83	0.83	0.51	0.38	0.51	-0.38	0.87	0.87
		Sag	-0.09	0.20	0.20	0.71	0.45	0.71	-0.03	0.24	0.24	0.54	0.29	0.54
P08	S1	Cor	0.33	0.36	0.36	0.29	0.47	0.47	0.30	0.41	0.41	0.27	0.47	0.47
		Sag	-0.27	-0.19	-0.27	0.18	-0.32	-0.32	-0.26	-0.16	-0.26	0.22	-0.33	-0.33
P08	S2	Cor	0.39	0.54	0.54	0.55	0.17	0.55	0.43	0.51	0.51	0.55	0.13	0.55
		Sag	0.09	-0.69	-0.69	-0.37	-0.32	-0.37	0.19	-0.61	-0.61	-0.37	-0.31	-0.37
P09	S1	Cor	0.49	-0.24	0.49	0.77	-0.39	0.77	0.56	-0.27	0.56	0.76	-0.44	0.76
		Sag	0.59	-0.12	0.59	0.70	0.30	0.70	0.61	-0.01	0.61	0.85	0.18	0.85

P09	S2	Cor	0.39	-0.09	0.39	0.64	-0.28	0.64	0.49	-0.01	0.49	0.77	-0.29	0.77
		Sag	0.38	0.23	0.38	0.72	0.67	0.72	0.40	0.32	0.40	0.78	0.69	0.78
P10	S1	Cor	0.32	0.14	0.32	0.47	-0.14	0.47	0.25	0.10	0.25	0.54	-0.15	0.54
		Sag	0.54	-0.32	0.54	0.54	0.49	0.54	0.53	-0.38	0.53	0.58	0.52	0.58
P10	S2	Cor	0.27	-0.04	0.27	0.47	0.27	0.47	0.33	-0.05	0.33	0.49	0.21	0.49
		Sag	0.43	-0.34	0.43	0.38	-0.34	0.38	0.40	-0.27	0.40	0.39	-0.42	-0.42
P11	S1	Cor	0.84	0.64	0.84	0.80	0.21	0.80	0.80	0.53	0.80	0.80	0.22	0.80
		Sag	0.58	0.36	0.58	0.70	0.07	0.70	0.70	0.36	0.70	0.80	-0.20	0.80
P12	S1	Cor	0.63	0.16	0.63	0.37	-0.26	0.37	0.71	0.08	0.71	0.66	-0.41	0.66
		Sag	0.25	0.53	0.53	0.37	0.31	0.37	0.40	0.41	0.41	0.35	0.34	0.35
P12	S2	Cor	0.73	-0.54	0.73	0.55	-0.25	0.55	0.75	-0.62	0.75	0.56	-0.20	0.56
		Sag	0.45	0.22	0.45	0.55	-0.01	0.55	0.52	0.23	0.52	0.60	-0.03	0.60
P13	S1	Cor	0.16	-0.01	0.16	0.14	0.21	0.21	0.00	0.14	0.14	0.22	0.20	0.22
		Sag	0.31	0.00	0.31	0.35	-0.02	0.35	0.48	0.00	0.48	0.36	-0.02	0.36
P13	S2	Cor	-0.06	-0.36	-0.36	0.02	0.06	0.06	-0.06	-0.33	-0.33	0.01	0.16	0.16
		Sag	0.30	-0.10	0.30	-0.37	-0.04	-0.37	0.42	-0.19	0.42	-0.37	-0.09	-0.37
Min/Max			-0.79/0.93			-0.79/0.89			-0.76/0.92			-0.81/0.90		
Absolute mean			0.53			0.59			0.55			0.62		
STD			0.49			0.54			0.52			0.54		
<i>p</i>			= 0.12									= 0.02		

Table 2. The correlation of abdomen-tumor and diaphragm-tumor with adjusted phase shifts. *p*: a Wilcoxon signed rank test with the absolute mean value for the correlation and the mean value for the phase shifts between FB and AV biofeedback.

Quantitative comparison		Abdomen-tumor correlation		Diaphragm-tumor correlation	
		FB	AV	FB	AV
Correlation	Min/Max	-0.82/0.96	-0.85/0.96	-0.82/0.93	-0.86/0.92
	Absolute mean	0.62	0.68	0.62	0.68
	STD	0.60	0.50	0.58	0.47
	<i>p</i>	= 0.01		< 0.01	
Phase shifts (s)	Min/Max	0.08/1.80	0.08/1.45	0.04/0.68	0.04/0.36
	Mean	0.32	0.30	0.20	0.17

STD	0.32	0.28	0.13	0.09
<i>p</i>	= 0.54		= 0.19	

Table 3. The correlation of abdomen-tumor and diaphragm-tumor with adjusted phase shifts across pre- and mid-treatment. Pre: pre-treatment, Mid: mid-treatment, Both: pre- and mid-treatment, and *p*: a Wilcoxon signed rank test between pre- and mid-treatment.

Quantitative comparison	Abdomen-tumor correlation						Diaphragm-tumor correlation						
	FB			AV			FB			AV			
	Pre	Mid	Both	Pre	Mid	Both	Pre	Mid	Both	Pre	Mid	Both	
Correlation	Min	-0.78	-0.77	-0.78	-0.85	-0.54	-0.85	-0.76	-0.74	-0.76	-0.86	-0.48	-0.86
	/Max	/0.96	/0.95	/0.96	/0.93	/0.96	/0.96	/0.93	/0.91	/0.93	/0.88	/0.92	/0.92
	Absolute mean	0.65	0.59	0.62	0.65	0.67	0.65	0.62	0.63	0.62	0.67	0.68	0.67
	STD	0.61	0.56	0.58	0.52	0.46	0.57	0.59	0.54	0.49	0.58	0.35	0.49
<i>p</i>	= 0.96			= 0.52			= 0.64			= 0.14			
Phase shifts (s)	Min	0.08	0.08	0.08	0.08	0.08	0.08	0.04	0.04	0.04	0.04	0.04	0.04
	/Max	/1.06	/1.80	/1.80	/0.92	/1.45	/1.45	/0.32	/0.44	/0.44	/0.36	/0.36	/0.36
	Mean	0.27	0.35	0.31	0.31	0.33	0.32	0.17	0.20	0.19	0.18	0.16	0.17
	STD	0.26	0.42	0.34	0.25	0.39	0.31	0.10	0.13	0.11	0.11	0.09	0.10
<i>p</i>	= 0.08			= 0.60			= 0.20			= 0.40			

Table 4. The correlation of abdomen-tumor and diaphragm-tumor with adjusted phase shifts and ≥ 5 mm tumor motion range. *p*: a Wilcoxon signed rank test between FB and AV biofeedback.

Quantitative comparison	Abdomen-tumor correlation		Diaphragm-tumor correlation	
	FB	AV	FB	AV
Min/Max	-0.82/0.96	-0.85/0.96	-0.82/0.93	-0.85/0.92
Absolute mean	0.67	0.75	0.68	0.76
STD	0.62	0.46	0.61	0.45
<i>p</i>	= 0.02		< 0.01	

